ELSEVIER

Journal of Neuroscience Methods 63 (1995) 175–183

JOURNAL OF NEUROSCIENCE METHODS

# Toward the ultimate metal microelectrode

G.E. Loeb [a,*], R.A. Peck [a], J. Martyniuk [b]

[a] *Bio-Medical Engineering Unit, Queen's University, Kingston, Kingston, Ont. K7L 3N6, Canada*
[b] *PI Medical Corporation, Portland, OR, USA*

Received 31 March 1995; accepted 29 July 1995

**Abstract**

The performance of metal microelectrodes for stimulating and recording neuronal action potentials depends on precise control of their geometrical, electrical and mechanical properties. We describe a combination of materials whose properties approach fundamental physical limitations on achievable performance and reproducible fabrication techniques that provide probes with very small dimensions. Pure iridium wire is electrolytically sharpened, vapor-coated with Parylene-C insulation and the tip exposed using an automatically steerable UV laser. Electrochemical activation of the iridium increases the capacitance of the metal-electrolyte interface so that the overall impedance in the relevant frequency band (100–10000 Hz) is dominated by the access resistance of the surrounding tissues.

*Keywords:* Electrophysiology; Parylene; Iridium

## 1. Background

Microelectrodes fabricated from sharpened wires have been a mainstay of neurophysiologists for over 40 years. Their narrow, tapering profiles permit them to be positioned very close to individual neurons in vivo, causing minimal damage as they pass through overlying tissues. They are usually insulated to within a few micrometers of the tip, which is used to record the highly localized extracellular potentials induced by action currents in one or a few of the neurons closest to the tip. They may also be used to inject highly localized stimulation currents to influence the excitability of the nearest neurons.

In the first 20 years of metal microelectrode use, scores of recipes for their fabrication were published (for reviews, see Loeb et al., 1977; Silver, 1987; for recent modifications, see Ashford et al., 1985; Quintana and Fuster, 1986; Abe, 1987; Millar and Williams, 1988; Worgotter and Eysel, 1988; Ciancone and Rebec, 1989; Jeanmonod et al., 1989; Jaeger et al., 1990; Jellema and Weijnen, 1991; Carter et al., 1992). More recently, most neurophysiologists have purchased commercially manufactured microelectrodes or have turned to intracellular techniques such as micropipettes and patch clamps. However, there remain a number of applications in which only extracellular microelectrodes can be used and in which the properties of commercial electrodes are less than optimal. Such applications include, in particular, penetrating tough connective tissue such as dura mater, recording from very small neurons, making multiple electrolytic lesions to mark recording sites in a penetration, microstimulating chronically without electrochemical damage, and identifying correlated activity from several identical and accurately spaced sites. We here present a combination of materials and technologies that can be used to build highly reproducible and reliable microelectrodes with properties approaching fundamental physical limits.

## 2. Requirements

### 2.1. Stimulation

Converting electrical current from the motion of electrons in a metal conductor to the motion of ions in an aqueous conductor requires electrochemical reactions. If the particular reactions that occur are fully reversible, then stimulation with biphasic pulses will result in no net changes in the metal surface and the surrounding tissues. Irreversible reactions lead inexorably to the accumulation of products, manifest as gas bubbles, pH shifts, and/or metal ion release; even small quantities of such products

* Corresponding author: Abramsky Hall, Queen's University, Kingston, Ont. K7L 3N6, Canada. Tel.: (613) 545-2790; Fax: (613) 545-6802; E-mail: LOEB@BIOMED.QUEENSU.CA.

Elsevier Science B.V.
*SSDI* 0165-0270(95)00107-7

may damage the immediately adjacent neurons that are the target of the stimulation.

Fortunately, the irreversible reactions all have threshold electromotive potentials that must be reached before they can occur at any appreciable rate, while the reversible reactions consist of capacitor-like reactions such as double-layer charging and hydrogen ion absorption that proceed in simple proportion to the applied voltage (for review, see Loeb et al., 1982). Unfortunately, the charge-carrying capacity of these reversible reactions tends to be proportional to the exposed surface area of the metal/electrolyte interface, which must be kept quite small to provide geometrical selectivity. Thus, the metal–electrolyte interface should be designed to maximize the amount of charge that can be injected into a given site before voltages must be applied that would exceed the threshold for irreversible electrochemical reactions.

It is worth noting that the ability to inject a particular amount of charge with a lower excursion in voltage is electrically equivalent to saying that the electrode requires less power. In certain applications such as neural prostheses (Loeb, 1989; Adler et al., 1990; Del Bufalo et al., 1993), the power dissipated by the metal–electrolyte interface itself may be a limiting factor in the selection and ultimate performance of the technologies used to store and transmit operating power to such devices.

### 2.2. Recording

The same electrochemical processes apply during recording of bioelectric potentials, except that the extremely low voltages (typically less than 1 mV) limit the available reactions to reversible, capacitor-like conductances and usually require even smaller tip geometries to approach the surface of the target cell membrane as closely as possible. In this case, the small surface area of the tip acts like a low-value capacitor in series with the electrical resistance of the immediately surrounding, moderately conductive saline. The resulting high-impedance value is associated with thermal noise that is proportional to the square root of the product of temperature, signal bandwidth and electrical impedance. (Technically, this Johnson-type thermal noise is associated with only the resistive and not the reactive component of the impedance, but the metal–electrolyte interface that gives rise to the capacitance is associated with thermal motion of the electrons and ions on either side of the double-layer that induces voltage noise similar to that in the resistive component; see also Millar and Williams, 1988.) High source impedance is also associated with a propensity to pick up extraneous noise by inductive and capacitive coupling of signals from other electromagnetic sources such as motors, lights and radio transmitters. When noise is superimposed on the bioelectric potentials, it confounds their interpretation, particularly in the common application of discriminating the similar waveforms generated by action potentials from several different neurons near a given microelectrode tip. Improvements in amplifier technology have greatly reduced the noise that their electronics add to the input signal (e.g., Szabo and Marczynski, 1993), so that noise associated with the microelectrode itself is often the limiting factor in the overall signal-to-noise ratio. Thus, the metal–electrolyte interface should be designed to have as low an impedance as possible for a given geometric tip size.

### 2.3. Mechanical

The metal microelectrode should be as slender as possible to minimize disruption of tissue along its insertion path but it must be stiff enough so that the tip will not be deformed and the shank will follow a straight track even when inserted through mechanically tough materials such as epineurium and dura mater (Goldstein and Salcman, 1973). This is particularly important when several closely and accurately spaced probes are desired. The insulating coating should be no thicker than necessary to avoid scratches and pinholes and ensure that the stray capacitance between the shank and any surrounding conductive fluids presents an impedance that is much higher than the tip impedance (to avoid dissipating recorded signals or stimulation currents). The profile should be smoothly tapered to avoid snagging on tissue during penetration, which is associated with 'dimpling' and local pressure increases that may cut off capillary circulation to the neurons (Jarvilehto et al., 1986). The geometry of the exposed tip should be accurately and reproducibly controlled and should remain unchanged during use. Conditions of use include repeated penetrations through connective tissue and deliberate application of electrical currents that result in massive irreversible reactions at the tip to generate electrolytic lesions that mark the position of the electrode tip when viewed in histological sections of the tissue.

## 3. Materials and methods

We selected pure iridium metal (75 $\mu$m diameter hot-drawn wire, Engelhard) for three reasons. First, it is extremely stiff, with a Young's modulus of elasticity equal to 517 GPa (even higher than tungsten, another commonly used microelectrode material, with Young's modulus = 400 GPa). Second, it is highly resistant to corrosion even when stimulated at voltages in excess of the threshold for electrolysis of saline. Third, its surface can be electrochemically 'activated', thereby raising the maximum charge density that can be achieved without resorting to irreversible reactions (Rand and Woods, 1974; Robblee et al., 1983).

### 3.1. Etching

The chemical properties that confer stiffness and corrosion resistance on iridium also make it very difficult to

etch. Prolonged etching (many minutes) is required with an applied anodic or AC voltage to induce electrolytic corrosion. This can be done in saturated sodium chloride (as suggested by Leo Bullara, Huntington Research Institute), which produces a relatively smooth surface that is useful for very fine electrodes with thin insulating coatings and small tip exposures (Fig. 1), or in saturated cyanide solution (in 30% sodium hydroxide), which produces a relatively rough surface that tends to increase the available surface area (Fig. 2). If the wire is dipped vertically in the solution (particularly for cyanide etching), the resultant electrolysis bubbles may interact with the elongated crystalline grain structure of drawn iridium wire to produce a very irregular 'moth-eaten' profile. We discovered that this problem could be eliminated by rotating the wire axially at 55 r.p.m. during etching. Depending on the desired taper, the wire may be left at a fixed depth or continuously dipped up and down with a one minute cycle (Bak Electronics Model EE-1D electrode etcher). Typical microelectrode tapers shown in Figs. 1 and 2 were etched from 75 $\mu$m diameter wire stock (the thinnest generally available commercially) by applying 6–8 VAC (60 Hz) for 7–9 min

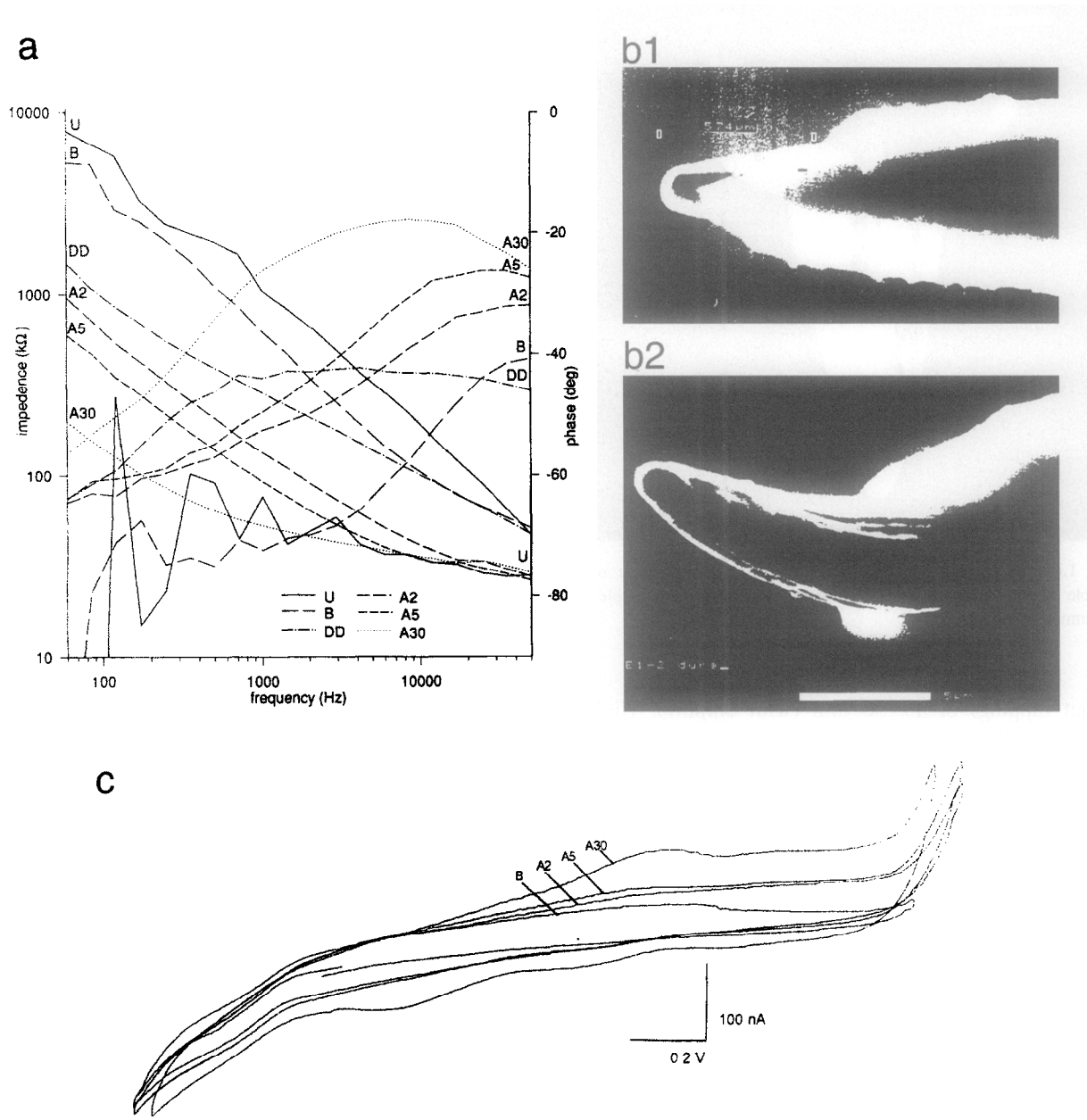


Fig. 1. a: impedance spectroscopy of a very fine-tipped iridium microelectrode suitable for single-unit recording, as shown in b1 before and b2 after being pushed twice through cat dura mater. Trace pairs show impedance magnitude (left ordinate and labels) and phase angle (right ordinate and labels) for unaltered surface after UV-laser exposure of tip (U), after cathodal electrolytic cleaning in phosphate-buffered saline (B), activation by cyclic voltammetry for 2, 5 and 30 min (A2, A5, and A30, respectively), and after 12 h air drying plus pushing through dura (DD); c: shows cycle voltammograms for conditions B, A2, A5 and A30.

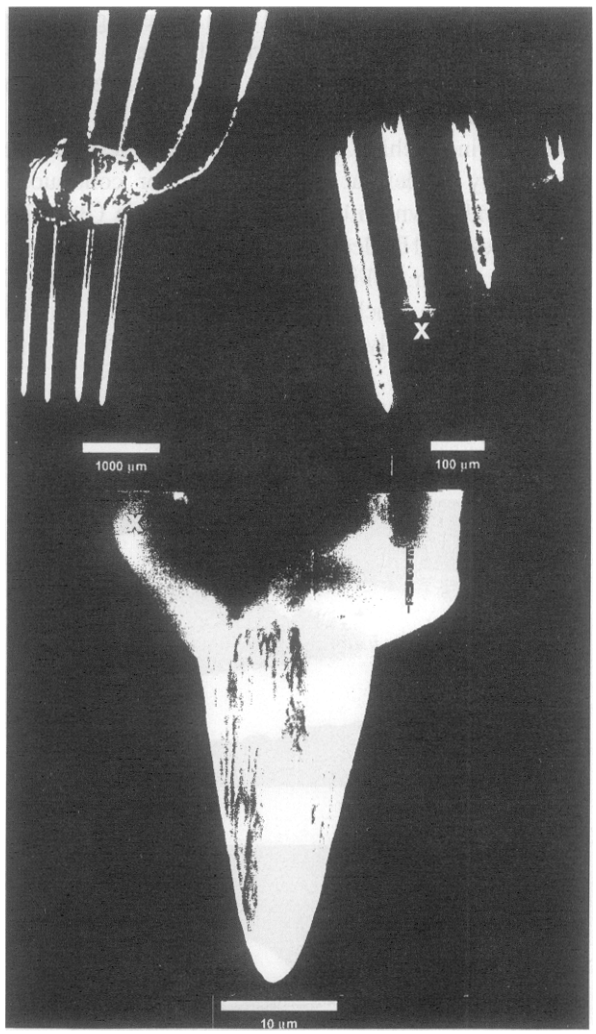


Fig. 2. Light micrograph (top left) and ESEM details of tips of a quadruple array of matched, relatively coarse microelectrodes suitable for microstimulation of cortex.

(without dipping) or 19–30 min (with dipping). Highly reproducible dimensions and shapes could be produced by a particular set of parameters.

### 3.2. *Insulating*

Parylene-C (poly-dichloro-diparaxylylene) is a biocompatible polymer that has been used commercially for microelectrodes (Micro Probe, Clarksburg, MD; A-M Systems, Toledo, OH) because its vapor deposition process lends itself well to precise thickness, pinhole-free coating of large batches of sharpened wires (Loeb et al., 1977). All of the microelectrodes described in this report were coated with thicknesses of 0.5–13 $\mu$m in a chamber built and operated to the exact specifications of the original Union Carbide chamber (described in Loeb et al., 1977). Chamber pressure was monitored during coating to assure that it remained under 80 $\mu$m of Hg (as measured by a thermister gauge operated at a local ambient temperature of 280°C to prevent fouling). Thickness was monitored during coating by the resonant frequency of a piezoelectric crystal (M-Tron MP-1 4 MHz) removed from its case and exposed to the plasma in the coating chamber at room temperature. Thickness was calibrated by IR spectroscopy and direct measurement of coating thickness in the environmental scanning electron microscope (ESEM Model E-3, ElectroScan, Wilmington, MA) used to characterize completed microelectrodes.

Over the past decade, there have been anecdotal reports of problems achieving mechanically and electrically robust coatings with commercial coating chambers. In a series of experiments with our own and various commercial coaters (unpublished data), we eventually traced this problem to the ratio of volume to surface area in the chambers. Briefly, the Parylene monomer requires about 10 000 collisions before it bonds to a site on another Parylene molecule, which accounts for its very even coating of complex contours. When a large-volume commercial chamber is operated with only a few test components for coating (a common practice for prototyping), the monomers are more likely to bond to each other in the gas phase than to join the growing polymer on the surfaces to be coated. The oligomers thus formed are eventually incorporated into the coating, resulting in a grainy, milky-appearing film that is mechanically friable and that is readily degraded in vivo by the action of macrophage. Similarly defective coatings occur when a normal chamber is operated at too high a plasma pressure (Schmidt et al., 1988), presumably because the shortened mean-free-path also favors oligomer formation. This problem does not arise in the small experimental coater operated at well-controlled pressure; it can be avoided in a large coating chamber by filling the volume with dummy surfaces (and increasing the amount of dimer raw material proportionately).

### 3.3. *Tip exposure*

Precise removal of Parylene from the tip has been problematic in the past. It has usually been achieved by applying a high voltage arc (about 4000 VDC) that first removes a cap of insulation by explosive ionization of gas trapped on the point of the metal tip and then burns back the desired length by sputter-etching in the corona (Loeb et al., 1977). The explosive arc cannot be used practically with coating thicknesses greater than 3 $\mu$m and it tends to loosen the Parylene adjacent to the tip, whose adhesion is derived solely from mechanical bonding. The square edges of the Parylene that are left by the corona discharge tend to snag on connective tissue and may crumple proximally from the tip, greatly increasing the effective tip exposure. The corona also tends to etch the iridium metal, blunting the tip and smoothing the microtexture of the surface that contributes importantly to the effective surface area. Plasma etching of Parylene has been described (Levy et al., 1986), but it requires physical masking that is difficult to do on very fine conical tips.

We used an ultraviolet laser beam (266 nm, frequency quadrupled Nd-YAG, Electroscientific Industries, Portland, OR) whose intensity was electronically controlled (Q-switched 1–500 mW), tightly focussed and automatically steered on a preprogrammed trajectory. As discussed in a preliminary report by Martyniuk et al. (1994) polymers can be ablated from refractory substrates by any laser beam with sufficient intensity, but the physics of wave motion results in a residual layer less than 1/2 wavelength thick that cannot absorb energy from the standing wave set up by the reflection from the metallic substrate. UV light is absorbed by metals such as iridum, raising its surface temperature to a level sufficient to ablate this residual layer and cleanly expose the metal surface. The beam intensity and dwell time can be programmed to remove the Parylene to a controlled depth in order to taper the edges of the coating adjacent to the tip. The coating on the far side of the tip from the beam is shadowed by the metal and must be removed by a second or reflected beam or by physically rotating the microelectrode and repeating the exposure process, as was done for this study.

### 3.4. Activation

By cycling the iridium metal between the anodic and cathodic voltages at which electrolysis begins, it is possible to build up a layer of iridium oxide to a desired thickness. Iridium oxide is electrically conductive, porous to hydroxyl ions, and exhibits a continuously variable stoichiometry that ranges from $Ir^{+3}$ to $Ir^{+4.8}$ (Huppauff and Lengeler, 1993). This means that each iridium atom in the layer acts like its own double-layer capacitor, capable of reversibly cycling at least 1 electron and 1 hydroxyl ion in and out of the metal and electrolyte, respectively. The effective charge-carrying capacity is thus multiplied by the number of monolayers of iridium oxide over that achievable by the bare metal surface. The useful thickness is limited by the access resistance of the electrolyte. Once the capacitive impedance of the iridium oxide becomes small compared to the resistances up to and within the oxide, further activation is ineffective and may even be counterproductive. The resistivity of iridium oxide is low for polarizations over the range $\pm 0.4$ V (with respect to a calomel reference electrode) but it increases exponentially with increasingly cathodic potentials (Glarum and Marshall, 1993).

We used a triangular waveform with a slope of 0.5 V/s (BioAnalytic Systems Model CV-27 equipped with Model PA-1 preamplifier) for various periods of time, while continuously monitoring the current–voltage profile (Fig. 1C) whose enclosed area represents charge-carrying capacity (Brummer et al., 1983). The voltage limits were adjusted manually for each electrode to the values at which electrolysis of water just begins (about $\pm 0.8$ VDC vs. calomel reference electrode, where current starts to increase rapidly in the voltammogram). An alternative, faster process using 1 Hz square waves with fixed voltage ranges has been described recently (Robblee et al., 1993). We preferred to use the traditional triangular waveform because we often found it necessary to adjust the positive and negative voltage limits individually for each electrode and occasionally during the activation process. This was particularly true for very fine tips ($< 10$ $\mu$m long or $50^2$ $\mu$m exposures), which could require applied voltages as high as $\pm 1.2$ V to reach electrolysis as determined by the sudden increase in current at either end of the voltage excursion. For such electrodes, the higher access resistance through the saline in series with the tip acts like a voltage divider, so a considerable overvoltage is required at the generator output to reach the necessary voltage drop across the metal–electrolyte interface.

### 3.5. Parallel arrays

Fig. 2 shows an array of 4 identical, separately connected microelectrode tips designed to be positioned at identical, calibrated depths (2 mm) and intertip spacings (0.4 mm) in the visual cortex for long-term microstimulation and recording in a freely moving subject (Salcman and Bak, 1976; Loeb et al., 1977; Schmidt et al., 1988). After electrolytic pointing of the iridium wire, each shank was gold-plated using a handheld pen (Gesswein) and welded to a 25 $\mu$m diameter gold wire at a measured distance from the tip. Melting a small gold ball on the end of the wire facilitated creating a resistance weld (Unitek Thinline weldhead at lowest power and pressure settings) without weakening the ultraflexible wire; a full wrap of wire around the shaft and a small drop of Stycast 1266 clear epoxy further strain-relieved the joint. The butt-ends of the iridium shafts were set into art gum to hold them in position as the shafts and tips were aligned by hand under a dissecting microscope. More epoxy was added to bridge the weld sites into a rigid backbone, the iridium shafts were cut off close to the cured epoxy and a final thin coat of epoxy was placed over the cut ends. The entire assembly was Parylene coated (6 $\mu$m thickness), covering the iridium tips, shanks, epoxy and individual gold leads with a conformal, pin-hole free coating. The tips were exposed by aligning each in succession in the path of the automatically steered laser beam.

### 3.6. Characterization

Individual microelectrodes were examined visually at various stages in their manufacture and testing using the environmental scanning electron microscope (ESEM). This type of SEM subjects the sample to low-pressure water vapor instead of a high vacuum. No particular sample cleaning or surface preparation is required; the usual tendency of nonconductive surfaces to absorb static charge is eliminated by the water vapor so that no metal vapor coating was required to resolve details of the Parylene

surface clearly. The rapid cycling of the chamber and non-destructive nature of the examination greatly facilitated serial measurements on single specimens.

Impedance spectroscopy was performed before and after growing different thicknesses of iridium oxide on the metal tips by successive periods of cycling as described above (Fig. 1A). In some cases, the iridium oxide was stripped from the surface by cathodic bubbling of the microelectrode at 9 VDC and the process repeated. A microelectrode tip could be repeatedly cycled in this way with no apparent changes in the impedance spectrogram resulting from a particular period of reactivation.

The test signals for spectroscopy were sinusoids ($\pm 0.1$ V, 60–50 000 Hz) with respect to a large indifferent electrode (platinum foil), generated by a Voltech Model TF2000 spectrum analyzer. We monitored the electrode current through a 1 k$\Omega$ resistor in series with the microelectrode rather than through the CVA-27 in order to avoid phase distortions produced by its low-pass filtering.

We did not attempt to clamp the polarization voltage of the microelectrodes to any particular value but rather let them settle to the value that they assumed when used with the TF2000, whose signal generation and monitoring circuitry is not unlike that used in conventional physiological amplifiers, stimulators and impedance monitors. Occasional measurements of polarization during characterization produced values between $\pm 0.05$ VDC with respect to a calomel reference electrode. Immediately after activation, polarization values were generally much higher and appeared to relax toward zero with a time constant of a few seconds. Impedance spectroscopy values measured before settling were often unstable and were discarded. Application of AC or DC test signals greater than $\pm 0.5$ V also produced unstable results, as would be expected from changes in the resistivity of iridium oxide (Burke and Whelan, 1984; Glarum and Marshall, 1993) and from the effects of electrolysis.

## 4. Results

### 4.1. Appearance

As shown in Figs. 1 and 2, the exposed metal surface showed a longitudinally rilled surface that appears to reflect the effects of electrolytic etching on the crystal structure of the metal. Occasionally, a somewhat coarser irregularity was seen, apparently reflecting a tendency for the drawn wire to have a small void near its center (M.J. Bak, personal communication). Laser exposure, electrochemical activation, electrolytic stripping of the oxide and mechanical penetration of test materials all had no discernible effect on this surface texture.

The Parylene coating was essentially featureless except for slight longitudinal undulations corresponding to the

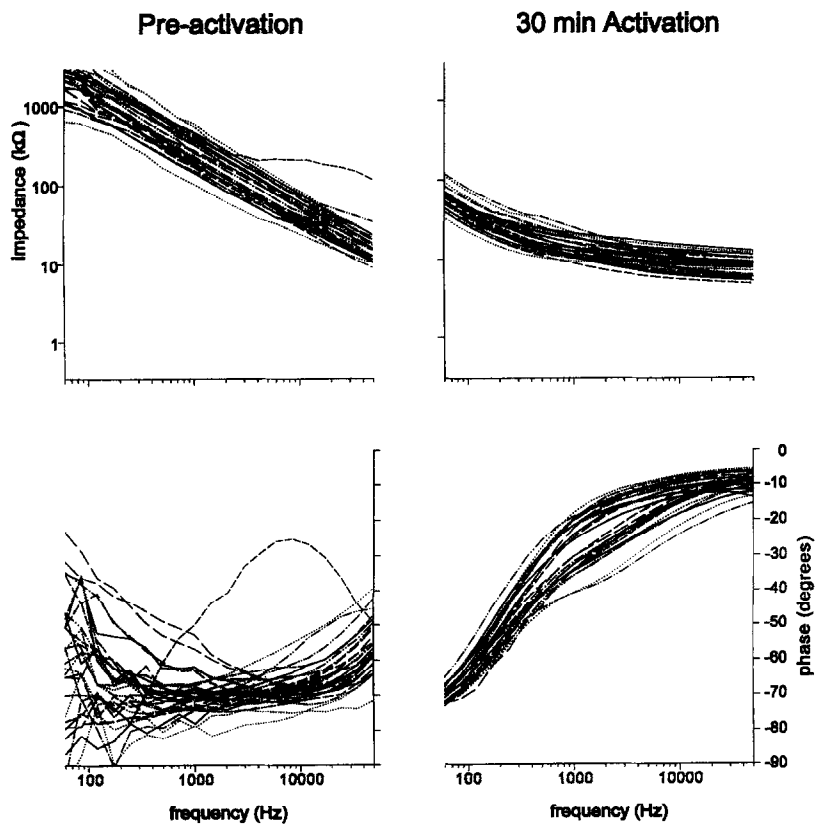


Fig. 3. Pre- (left) and post-activation (right) impedance spectrograms (magnitudes at top, phases at bottom) for 24 matched microelectrodes similar to that shown in Fig. 2.

deeper rills in the underlying metal. There was a slight texturing of the surface that was tapered by the laser beam. The seam between the edge of the Parylene and the exposed tip appeared to be tightly adherent, although slightly undercut in some views. The edges were slightly rounded and a small amount of debris could occasionally be seen on the shoulders, presumably from redeposition of ablated material. Stepped and tapered profiles could be produced reproducibly in the thicker coatings by appropriate programming of the beam power, course and speed. Failure to align the beam identically for the two exposures required to strip both sides of the tip occasionally resulted in the asymmetrical profile shown in Fig. 1b1.

### 4.2. Impedance

Impedance spectroscopy consistently provided sufficient information to distinguish the effects of the size of the exposed tip from the effects of various electrochemical states of the iridium metal. Fig. 1a shows the family of curves obtained for the very fine microelectrode shown in Fig. 1b. In the unactivated state (U; as received after laser stripping), the impedance is high and the phase angle noisy and inconsistent from sweep to sweep. Conventional cathodic bubbling to clean the tip (B; −3 VDC for 10 s) produced only a small decrement in magnitude, indicating that the tip was cleanly exposed down to the iridium surface by the laser process. The initial sweep of the cyclic voltammogram (B in Fig. 1c) shows a relatively featureless contour typical of simple double-layer charging. Activation for periods of 2, 5 and 30 min (traces A2, A5 and A30, respectively) led gradually to the bumpy, asymmetrical shape associated with the various valence-states of iridium oxide. The corresponding impedance spectrograms all asymptote at a similarly low impedance value ($\approx 30\ k\Omega$) and predominantly resistive phase angle ($\approx -20°$) at the highest frequencies. All of these curves are similar to simple high-pass filters with progressively lower cut-off frequencies, presumably the result of progressively larger amounts of capacitive conductance from the accumulating thickness of iridium oxide in series with the fixed resistance of the surrounding saline.

The impedance magnitude at 1 kHz (a value often used to characterize metal microelectrodes) correlated well with the extent of tip exposure revealed by ESEM, but only when the iridium surfaces were in similar electrochemical states. For the microelectrode arrays shown in Fig. 2, we required a large number of larger, well-matched tips. Fig. 3 shows the impedance spectroscopy after bubbling for a few seconds at −9 VDC to clean the tips (pre-activation)

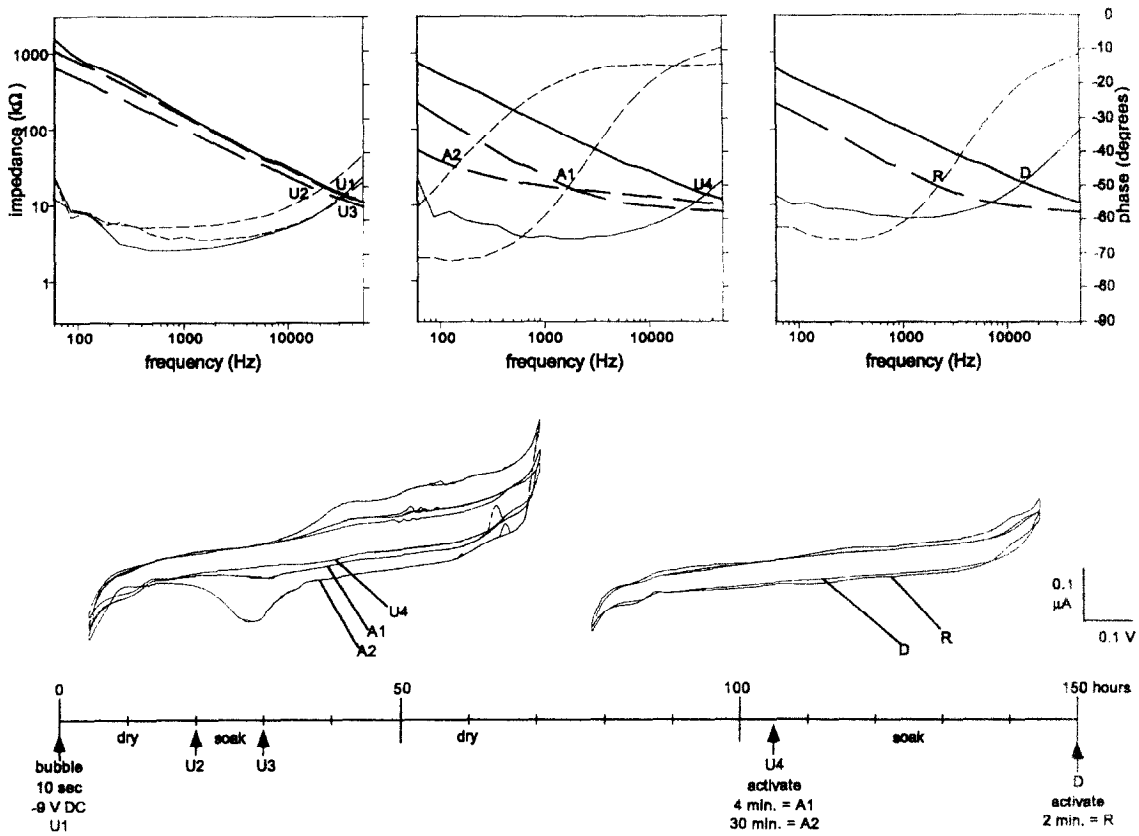


Fig. 4. Impedance spectroscopy (top row) and cyclic voltammograms (middle row; calibrations at far right) for microelectrode shown in Fig. 2 for various conditions indicated on timeline at bottom. U1-4 are preactivation conditions after various periods of air drying and soaking in phosphate-buffered saline; A1-2 are initial results of 4 and 30 min activation, respectively; D is spontaneous deactivation after 42 h soaking in saline and R is result of 2 min of reactivation.

and after 30 min of activation for a set of 24 identical microelectrodes. The impedance magnitudes were quite homogeneous for all electrodes and decreased by about a factor of 10 at 1 kHz. The impedance spectrum of the unactivated iridium was similar to that reported for platinum in that the magnitude decreased less than proportionately with increasing frequency and the phase angle was relatively constant across frequencies, although quite inconsistent from electrode to electrode. By contrast, the activated iridium acted like a large, fixed value capacitor in series with a fixed resistor across all frequencies, resulting in a plot similar to a high-pass filter with a cut-off frequency of around 300 Hz. For frequencies above this value, the impedance was a nearly pure resistance presumably associated with the access resistance of the saline surrounding the tip.

### 4.3. Mechanical robustness

We subjected various microelectrode designs (0.5–13 $\mu$m thickness insulation, 5–30 $\mu$m tip exposures) to a series of mechanical and electrochemical tests that are generally quite destructive for conventional microelectrodes. Even for conditions at the limits of usual conditions of use (e.g., penetrating connective tissue, pushing into the skin of an orange, anodal-lesioning to mark recording sites, etc.), no changes were detectable visually. Even direct contact of the tips with hard objects often resulted in only minimal hooking of the most distal part of the tip rather than permanent bending of the tapered or straight regions of the shaft. Application of large cathodal currents through the tip tended to strip the activation layer over a period of many seconds, but this could be restored to its original state by repeating the cycling process.

We and others have noted that penetrating dura mater tends to be particularly hard on microelectrodes. Fig. 1b shows a very fine microelectrode with 1 $\mu$m thick Parylene insulation before (b1) and after (b2) two penetrations of fresh cat dura mater. The iridium metal has been bent; the Parylene insulation is still snug around the base of the cone but appears to have been pushed back, approximately doubling the length of the original tip exposure. Paradoxically, this problem could be avoided by using thicker Parylene coatings (6–13 $\mu$m) despite the larger 'shoulder' that had to pass through the connective tissue. Presumably this is because the thicker layer better resisted the circumferential stretching required to push the Parylene away from the conical tip; the sloped shoulders (see Fig. 2) of the relatively soft but high tensile-strength polymer apparently deformed as they passed through the connective tissue.

### 4.4. Electrochemical stability

Perhaps the main disadvantage of these electrodes was the uncertainty about how long the activated state would persist under different conditions of use and storage. The activated tip impedances were remarkably stable for periods of several hours of immersion testing and for brief periods of drying and rinsing in distilled water, as long as the small tip surface was not fouled by dust or oil as it passed in and out of the solutions. However, as shown in Figs. 1 and 4, the microelectrodes occasionally appeared to lose virtually all of their activation spontaneously after many hours of disuse in either the dry or wet states. These switched off electrodes reverted to cycle voltammograms and impedance spectrograms typical of the clean but unactivated iridium (see traces D in Fig. 4). When subjected to voltage scans to reactivate them, they showed no signs of their previous activation, going through the usual slow build-up of features in their voltammograms (traces R in Fig. 4). Fig. 1a illustrates the ambiguity that results from trying to use impedance magnitude to track microelectrode condition when mechanical damage increases tip exposure (ESEM b1 vs. b2) simultaneously with a change of electrochemical state. The paradoxical increase in tip impedance can be explained by noting the larger phase lag that persists across all frequencies, indicating that the previously activated region of the old tip (electrically in parallel with the newly exposed iridium) is no longer any more activated than the newly exposed surface.

## 5. Discussion

The fabrication processes described herein provide precise and reproducible techniques to build electrodes with virtually any required dimensions from materials that provide the best known properties that can be achieved physically. Parylene has dielectric, mechanical and biocompatibility properties that are equal or superior to virtually every known polymer that can be applied as a coating on wires. Inability to precisely contour and remove this material from a tip without disrupting its mechanical adhesion to the substrate has been the main limitation to its use in the past. Iridium has mechanical stiffness and corrosion resistance near the limits of all known metals. Inability to reliably etch it into fine tips from relatively large wire stock has been the main limitation to its use. The methods described here overcome both limitations.

The activation process can be tuned to achieve an optimal thickness in which the limiting factor for electrode impedance and charge injection is the irreducible resistivity of the saline in and around the porous oxide layer. Once the activation reaches a thickness where the impedance at the relevant frequency approaches zero phase angle, the only way to reduce impedance further is to enlarge the geometrical surface, which changes the selectivity of neural recording and stimulation. Determining the actual sizes and tapers for the exposed tip and insulated shank that perform optimally in a particular electrophysiological application will require systematic experimentation, a process that can now proceed with the tools at hand.

Instability of iridium activation has been noted by others and is under investigation (Robblee et al., 1993). It has not been described in chronic animal tests of pacemaker electrodes (Adler et al., 1990), but that application involved much larger surface areas and much smaller decreases in measured impedance over conventional metal–electrolyte interfaces. Unless and until the deactivation problem can be overcome for typical conditions of storage, sterilization and chronic use, it will be important to activate the iridium as close to the time of use as possible. It seems likely that this can be accomplished efficiently and safely even in vivo by a relatively simple potentiostatic oscillator. For very small tips, however, special care will need to be taken to make sure that sufficient voltage excursions are available to achieve activation without causing frank electrolysis. It remains to be seen if such tips, once activated, can be maintained in a stable state by some routine of low-level stimulation. Impedance spectroscopy (with particular attention to phase angle as well as magnitude plots vs. frequency) seems to be a particularly valuable tool for assessing the degree of activation of the iridium microelectrode tips and their consequent electrical properties in recording and stimulation applications. Conventional single impedance magnitudes at 1 kHz cannot distinguish between changes in activation and damage to or partial fouling of an activated tip.

## Acknowledgements

The authors thank Martin J. Bak of the US National Institutes of Health and Lois Robblee of EIC Laboratories for many helpful discussions of electrode technology over the years.

## References

Abe, T. (1987) Fabrication method for multimicroelectrodes using quartz glass as insulator material. [Japanese: Iyodenshi. to. Seitai. Kogaku.], Jpn J. Med. Electron. Biol. Eng., 25: 299–301.

Adler, S., Spehr, P., Allen, J. and Block, W. (1990) Chronic animal testing of new cardiac pacing electrodes, Pace. Pac. Clin Electrophys., 13: 1896–1900.

Ashford, J.W., Coburn, K.L. and Fuster, J.M. (1985) The elgiloy microelectrode: fabrication techniques and characteristics, J. Neurosci. Methods, 14: 247–252.

Brummer, S.B., Robblee, L.S. and Hambrecht, F.T. (1983) Criteria for selecting electrodes for electrical stimulation: Theoretical and practical considerations, Ann. NY Acad. Sci., 405: 159–171.

Burke, L.D. and Whelan, D.P. (1984) A voltammetric investigation of the charge storage reactions of hydrous iridium oxide layers, J. Electron. Chem., 162: 121–141.

Carter, S.J., Linker, C.J., Turkle-Huslig, T. and Howard, L.L. (1992) Comparison of impedance at the microelectrode-saline and microelectrode-culture medium interface, IEEE Trans. Biomed. Eng., 39: 1123–1129.

Ciancone, M.T. and Rebec, G.V. (1989) A simple device for the reliable production of varnish-insulated, high-impedance tungsten microelectrodes, J. Neurosci. Methods, 27: 77–79.

Del Bufalo, A.G., Schlaepfer, J., Fromer, M. and Kappenberger, L. (1993) Acute and long-term ventricular stimulation thresholds with a new, iridium oxide-coated electrode, Pace. Pacing. Clin. Electrophysiol., 16: 1240–1244.

Glarum, S.H. and Marshall, J.H. (1993) The A-C response of iridium oxide films, J. Electrochem. Soc., 127: 1467–1474.

Goldstein, S.R. and Salcman, M. (1973) Mechanical factors in the design of chronic recording intracortical microelectrodes, IEEE Trans. Biomed. Eng., 20: 260–269.

Huppauff, M. and Lengeler, B. (1993) Valency and structure of iridium in anodic iridium oxide films, J. Electrochem., 140. 598–601.

Jaeger, D., Gilman, S. and Aldridge, J.W. (1990) A multiwire microelectrode for single unit recording in deep brain structures, J. Neurosci. Methods, 32: 143–148.

Jarvilehto, M., Meinertzhagen, I.A. and Shaw, S.R. (1986) Anti-adhesive coating for glass microelectrodes, J. Neurosci. Methods, 17: 327–334.

Jeanmonod, D., Sindou, M., Magnin, M. and Boudet, M. (1989) Intra-operative unit recordings in the human dorsal horn with a simplified floating microelectrode. Electroenceph. Clin. Neurophysiol., 72: 450–454.

Jellema, T. and Weijnen, J.A.W.M. (1991) A slim needle-shaped multiwire microelectrode for intracerebral recording, J. Neurosci. Methods, 40: 203–209.

Levy, B.P., Campbell, S.L. and Rose, T.L. (1986) Definition of the geometric area of a microelectrode tip by plasma etching of Parylene, IEEE Trans. Biomed. Eng., 33: 1046–1049.

Loeb, G.E. (1989) Neural prosthetic interfaces with the nervous system, TINS, 12: 195–201.

Loeb, G.E., Bak, M.J., Salcman, M. and Schmidt, E.M. (1977) Parylene as a chronically stable, reproducible microelectrode insulator, IEEE Trans. Biomed. Eng., 24: 121–128.

Loeb, G.E., McHardy, J. and Kelliher, E.M. (1982) Neural prosthesis. In: D.F. Williams (Ed.), Biocompatibility in Clinical Practice, Vol. II, CRC Press, Boca Raton, FL, pp. 123–149.

Martyniuk, J., Corbett, S. and Loeb, G.E. (1994) UV laser based micromachining, Med. Dev. Diag. Industry, October 1944, pp. 110–121.

Millar, J. and Williams, G.V. (1988) Ultra-low noise silver-plated carbon fibre microelectrodes, J. Neurosci. Methods, 25: 59–62.

Quintana, J. and Fuster, J.M. (1986) A microelectrode for depth recording in awake animals, Electroenceph. Clin. Neurophysiol., 63: 83–85.

Rand, D.A.J. and Woods, R. (1974) Cyclic voltammetric studies on iridium electrodes in sulphuric acid solutions: nature of oxygen layer and metal dissolution, J. Electranal. Chem. Interfac. Electrochem., 55: 375–381.

Robblee, L.S., Cogan, S.F., Rose, T.L., Twardoch, M.U., Jones, G.S. and Jones, R.B. (1993) Studies of the Electrochemistry of Stimulating Electrodes, 8th Quart. Report 29 May 1993 to 28 August 1993. Contract #N01-NS-1-2300, pp. 1–25.

Robblee, L.S., Lefko, J.L. and Brummer, S.B. (1983) Activated Ir: an electrode suitable for reversible charge injection in saline solution, J. Electrochem. Soc., 130: 731–733.

Salcman, M. and Bak, M.J. (1976) A new chronic recording intracortical microelectrode, Med. Biol. Eng., 14: 42–54.

Schmidt, E.M., McIntosh, J.S. and Bak, M.J. (1988) Long-term implants of Parylene-C coated microelectrodes, Medical Biol. Eng. Comput., 26: 96–101.

Silver, I.A. (1987) Microelectrodes in medicine, Philosoph. Trans. Roy. Soc. Lond. Series. B, Biol. Sci., 316: 161–167.

Szabo, I. and Marczynski, T.J. (1993) A low-noise preamplifier for multisite recording of brain multi-unit activity in freely moving animals, J. Neurosci. Methods, 47: 33–38.

Worgotter, F. and Eysel, U.T. (1988) A simple glass-coated, fire-polished tungsten electrode with conductance adjustment using hydrofluoridic acid, J. Neurosci. Methods, 25: 135–138.